Plant Communications
Research Article

CellPress
Partner Journal

Rice OsUBR7 modulates plant height by regulating histone H2B monoubiquitination and cell proliferation

Yangyi Zheng[1,2], Sensen Zhang[1,2], Yanqiu Luo[1,2], Fuquan Li[1,2], Jiantao Tan[1,2], Bin Wang[1,2], Zhe Zhao[1,2], Huifang Lin[1,2], Tingting Zhang[1,2], Jianhong Liu[1,2], Xupeng Liu[1,2], Jingxin Guo[1,2], Xianrong Xie[1,2], Letian Chen[1,2], Yao-Guang Liu[1,2,*] and Zhizhan Chu[1,2,3,*]

[1]State Key Laboratory for Conservation and Utilization of Subtropical Agro-bioresources, College of Life Sciences, South China Agricultural University, Guangzhou 510642, China

[2]Guangdong Laboratory for Lingnan Modern Agriculture, Guangzhou 510642, China

[3]Guangdong Provincial Key Laboratory of Protein Function and Regulation in Agricultural Organisms, South China Agricultural University, Guangzhou 510642, China

***Correspondence: Yao-Guang Liu (ygliu@scau.edu.cn), Zhizhan Chu (chuben@scau.edu.cn)**

https://doi.org/10.1016/j.xplc.2022.100412

ABSTRACT

Plant height is an important agronomic trait for lodging resistance and yield. Here, we report a new plant-height-related gene, *OsUBR7* in rice (*Oryza sativa* L.); knockout of *OsUBR7* caused fewer cells in internodes, resulting in a semi-dwarf phenotype. *OsUBR7* encodes a putative E3 ligase containing a plant homeodomain finger and a ubiquitin protein ligase E3 component N-recognin 7 (UBR7) domain. OsUBR7 interacts with histones and monoubiquitinates H2B (H2Bub1) at lysine148 in coordination with the E2 conjugase OsUBC18. OsUBR7 mediates H2Bub1 at a number of chromatin loci for the normal expression of target genes, including cell-cycle-related and pleiotropic genes, consistent with the observation that cell-cycle progression was suppressed in the *osubr7* mutant owing to reductions in H2Bub1 and expression levels at these loci. The genetic divergence of *OsUBR7* alleles among *japonica* and *indica* cultivars affects their transcriptional activity, and these alleles may have undergone selection during rice domestication. Overall, our results reveal a novel mechanism that mediates H2Bub1 in plants, and *UBR7* orthologs could be utilized as an untapped epigenetic resource for crop improvement.

Keywords: histone H2B monoubiquitination, E3 ligase, UBR7, plant height, rice

Zheng Y., Zhang S., Luo Y., Li F., Tan J., Wang B., Zhao Z., Lin H., Zhang T., Liu J., Liu X., Guo J., Xie X., Chen L., Liu Y.-G., and Chu Z. (2022). Rice OsUBR7 modulates plant height by regulating histone H2B monoubiquitination and cell proliferation. Plant Comm. **3**, 100412.

INTRODUCTION

Asian rice (*Oryza sativa* L.) is a major staple crop that feeds over half of the world's population. In the 1960s, the utilization of semi-dwarf germplasm resources in wheat and rice breeding drastically improved lodging resistance and grain yield, resulting in the so-called "Green Revolution". The causal gene *SD1* in rice encodes the key enzyme GA20ox-2 essential for gibberellin biosynthesis, and its mutant *sd1* alleles confer the semi-dwarf trait (Monna et al., 2002; Sasaki et al., 2002; Spielmeyer et al., 2002). Over the past decades, extensive use of *sd1* alleles in rice breeding has also brought potential threats to rice production, such as germplasm homogenization and increasing risks of pathogen and insect attack (Gaur et al., 2020). Therefore, extensive efforts have been made to look for alternative semi-dwarf genes in rice breeding. A number of genes that regulate plant height and lodging resistance have been identified over the past few decades. These genes mostly encode transcriptional regulators and thus regulate a large number of downstream genes. As a result, functional disturbance of these genes, such as *OsLOL2* (Xu and He, 2007), *OsAP2-39* (Yaish et al., 2010), and *LAX* (Komatsu et al., 2003), often has pleiotropic negative effects on plant growth and grain yield (Gaur et al., 2020). Thus, searching for suitable new gene alleles that may confer ideal plant height and other beneficial traits for rice breeding has been a continuous goal.

Published by the Plant Communications Shanghai Editorial Office in association with Cell Press, an imprint of Elsevier Inc., on behalf of CSPB and CEMPS, CAS.

Epigenetic modifications, such as DNA methylation and histone modifications, play important roles in regulating diverse cellular processes and development in eukaryotes by regulating transcriptional activity. Epigenetic diversity controlled by protein-coding and non-coding genes may thus provide additional sources of variation for crop improvement (Kouzarides, 2007; Ahmad et al., 2010; He et al., 2011; Springer and Schmitz, 2017). Previous studies have shown that monoubiquitination of nucleosome core histones, which occurs mainly at lysine sites on histones H2A and H2B, positively regulates gene transcription and is involved in DNA-damage responses in animals (Joo et al., 2007; Weake and Workman, 2008; Richly et al., 2010; Ramanathan and Ye, 2012). H2B monoubiquitination (H2Bub1) requires the sequential actions of three enzymes. A Ub-activating enzyme (E1) activates ubiquitin (Ub) and forms a thioester bond between the Ub C terminus and the catalytic cysteine on the E1 protein. Ub is then transferred to the catalytic cysteine of one of ~40 Ub-conjugating enzymes (E2) and is finally transferred to the target lysine residue of H2B by a Ub E3 ligase (Robinson and Ardley, 2004; Braun and Madhani, 2012). Plant HISTONE MONOUBIQUITINATION1 (HUB1) and HUB2 proteins, such as *Arabidopsis thaliana* AtHUB1 and AtHUB2, tomato (*Solanum lycopersicum*) SlHUB1 and SlHUB2, and rice OsHUB1 and OsHUB2, similar to their human homologs RNF20 and RNF40, act as RING-type H2Bub1 E3 ligases and play important roles in regulation of chromatin epigenetic status, growth and development, and stress responses (Fuchs et al., 2012; Zhang et al., 2015; Zhao et al., 2019). A recent study reported a new type of H2Bub1 ligase in humans, ubiquitin protein ligase E3 component N-recognin 7 (UBR7). This type of E3 ligase uses its unique UBR7 zinc finger to monoubiquitinate H2B instead of relying on a RING zinc finger, functioning to suppress tumorigenesis and metastasis of breast tumors by regulating cell-adhesion genes (Adhikary et al., 2019). However, whether plant UBR7 homologs function in histone modification and play roles in regulating plant growth and development remains unclear.

In this study, we identified the rice gene *OsUBR7* that encodes a homolog of human UBR7. CRISPR–Cas9 knockout mutants of *OsUBR7* exhibited a semi-dwarf phenotype due to reduced cell numbers in the internodes. We demonstrated that OsUBR7 interacts specifically with the E2 conjugase OsUBC18 to function as an H2Bub1 E3 ligase at K148 site. We showed that H2Bub1 levels in the whole genome and at certain genomic loci were significantly reduced and that multiple cell-cycle-related genes were significantly downregulated, thus affecting cell proliferation in the *osubr7* mutant. Divergent alleles of this gene may have undergone selection during rice domestication. Our results reveal a novel epigenetic regulatory mechanism by which OsUBR7 functions as an H2BK148ub ligase and regulates plant height and other traits.

RESULTS

Characterization of a new semi-dwarf mutant in rice

During the development of a plant CRISPR–Cas9 genome-editing system, we created a mutant library of rice varieties by targeted mutagenesis of various genes using this system (Ma et al., 2015). Analysis of this mutant library revealed that targeted mutations of the gene *Os06g0529800/LOC_Os06g33810* in the rice cultivar Nipponbare (*O. sativa* ssp. *japonica*) resulted in reduced plant height compared with wild-type (WT) Nipponbare (Supplemental Figure 1A). We selected a homozygous mutant (T1-1) for further study. An F_2 family from a cross of T1-1 × Nipponbare showed a 3:1 segregation ratio for plant height (Supplemental Figure 1B), suggesting that the mutant phenotype was caused by a recessive mutation. Because *Os06g0529800* encodes a homolog of human UBR7 (see below), we named this gene *OsUBR7* and its mutant alleles *osubr7*. In addition to reduced plant height (~22 cm lower than the WT) (Figures 1A and 1B), the mutant plants also showed slightly decreased grain width, length, and weight and shorter leaf length but had increased tiller numbers (Supplemental Figure 2).

To further confirm that the mutations of *OsUBR7* indeed caused these phenotypic variations, we generated a genetic complementation construct containing the native *OsUBR7* locus (a 5901-bp genomic region including the 2256-bp promoter region and the 1228-bp downstream sequence from Nipponbare) and introduced it into the mutant line. The transgenic lines (T_2) *OsUBR7*^{t}#5 and *OsUBR7*^{t}#7 showed an obvious increase in plant height compared with the mutant (Supplemental Figures 3A–3C). We also transferred a construct with an *OsUBR7* cDNA-FLAG fusion driven by the maize (*Zea mays*) *Ubiquitin* promoter into the mutant line (Supplemental Figure 3D). The T_2 overexpression lines (*OsUBR7*^{OE}#5 and *OsUBR7*^{OE}#9) also displayed an obvious increase in plant height compared with the mutant (Supplemental Figures 3E–3H). Taken together, these results demonstrated that *OsUBR7* (*Os06g0529800*) indeed regulates rice plant height.

Rice plant height depends on the number and length of internodes, and internode length is determined by cell division and cell elongation in the intermediate meristem (Yamamuro et al., 2000; Wang and Li, 2008). To determine the reason for the semi-dwarf phenotype, we compared the *osubr7* mutant (in the Nipponbare background) with WT Nipponbare and found that they had the same number of internodes, but all were shortened in *osubr7* (Figures 1C and 1D). In addition, the basal internodes exhibited greater length reduction in *osubr7* (Figure 1E). Our observations of the second internodes (counting from the top) revealed that the average length of parenchyma cells did not differ significantly between *osubr7* and the WT (Figures 1F and 1G). This result suggested that the semi-dwarf phenotype of *osubr7* was due to the decreased number of internode cells. To confirm the observation of internode cells, we counted the epidermal cell numbers of the glumes (lemma) of mature grains from WT and *osubr7* under a scanning electron microscope. The results showed that total cell number along the longitudinal axis was reduced by 16.1% in *osubr7* grains compared with WT grains, but there were no significant differences in average epidermal cell length (Figures 1H–1K). These results confirmed that differences in internode and grain length between *osubr7* and WT were due mainly to differences in cell number in these tissues.

OsUBR7 encodes a putative nuclear-localized UBR7 finger-E3 ligase

Sequence analysis of cDNA obtained by reverse transcription PCR (RT–PCR) and rapid amplification of cDNA end PCR revealed that the *OsUBR7* cDNA is 1678 bp in length, with a

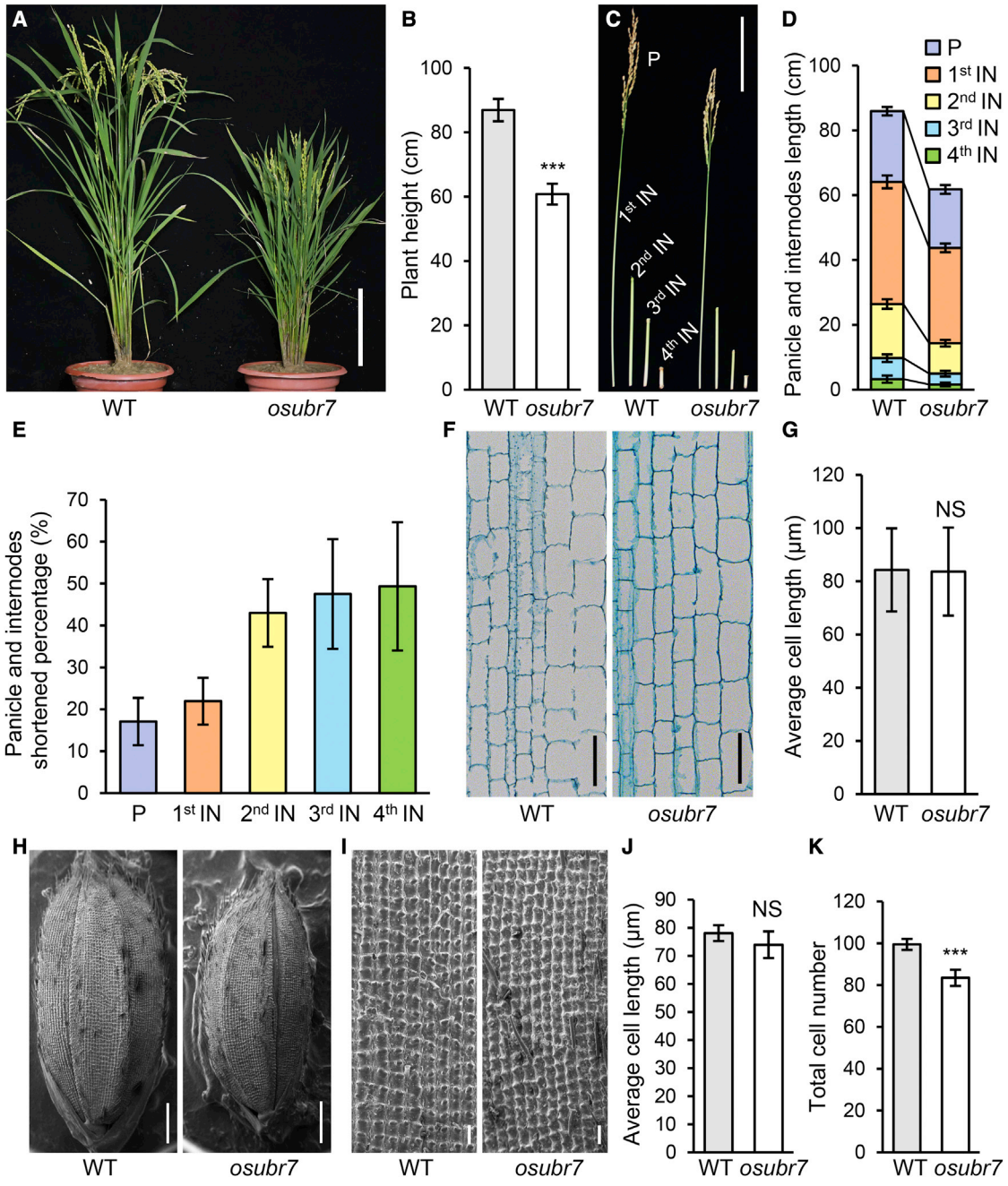

Figure 1. Decreased numbers of internode and glume cells lead to semi-dwarfing and smaller grains in *osubr7* plants.

(A) Phenotypes of wild-type (WT) and *osubr7* (T_4) plants. Scale bar, 20 cm.

(B) Comparison of plant height between WT and *osubr7*. Data are means ± SD (n = 30). ***p < 0.001 (Student's t-test).

(C) Phenotypes of culms in WT and *osubr7*. Scale bar, 10 cm.

(D) Panicle and internode length of culms in WT and *osubr7*. P, panicle; IN, internode. The number of internodes was counted from top to bottom. Data are means ± SD (n = 30).

(E) Percentage of panicle and internode height of *osubr7* compared with WT. Data are means ± SD (n = 30).

(F) Longitudinal sections from the second internode of WT and *osubr7*. Scale bars, 100 μm.

(G) Parenchyma cell length in the second internode of WT and *osubr7*. Data are means ± SD (n = 400 cells from three plants). NS, not significant.

(H and I) Scanning electron micrographs of the mature grain and lemma surfaces in WT and *osubr7*. Scale bars, 1 mm **(H)** and 100 μm **(I)**.

(J and K) Comparisons of average epidermal cell length **(J)** of lemma shown in **(I)** and total cell number **(K)** shown in **(H)**. Data are means ± SD (n = 4 biological repeats). ***p < 0.001 (Student's t-test). NS, not significant.

139-bp 5′ untranslated region (UTR) and a 276-bp 3′ UTR (Figure 2A). Its 1260-bp open reading frame encodes a putative UBR7 protein named OsUBR7 that contains a UBR-box domain and a PHD finger (Figure 2B; Supplemental Figures 4A and 4B).

The PHD domain in UBR7 proteins is known as a histone recognition motif (Kleiner et al., 2018; Adhikary et al., 2019; Longbotham et al., 2019). The zinc coordination folds of UBR7 and RING finger domains are highly similar, although the zinc-coordinating Cys158, His163, and His166 of the UBR7 zinc finger (which is stabilized by zinc ion coordination in a cross-braced topology) are different from the classical RING finger-E3 ligases (Supplemental Figures 5 and 6). Moreover, the UBR7 zinc finger is highly conserved among eukaryotes (Supplemental Figures 4B and 5), and human UBR7 functions as an H2BK120ub ligase (Adhikary et al., 2019). Therefore, we speculated that OsUBR7 may function as an E3 ligase with histone(s) as substrate(s).

We analyzed *OsUBR7* expression patterns via quantitative RT–PCR (qRT–PCR). *OsUBR7* was expressed in all organs and tissues examined (Figure 2C). In addition, we transferred a construct containing the native *OsUBR7* promoter (2256 bp including the 5′ UTR) fused to the β-glucuronidase (GUS) reporter gene into Nipponbare. The GUS signal was observed ubiquitously in the transgenic plants, including in root, leaf, leaf sheath, spikelets, pistils, stamen, glume, and stem (Figures 2D–2J). Subcellular localization with OsUBR7-GFP and GFP-OsUBR7 fusion proteins confirmed that OsUBR7 was localized in the nuclei (Figure 2K). Taken together, these results showed that *OsUBR7* is constitutively expressed and encodes a nuclear-localized protein, consistent with its presumed function in histone monoubiquitination.

H2B is a monoubiquitination substrate for OsUBR7

To identify candidate substrates modified by OsUBR7, we used a transgenic line (*OsUBR7*^{OE}#9) overexpressing an OsUBR7-FLAG fusion protein for co-immunoprecipitation (Co-IP). Liquid chromatography–tandem mass spectrometry (MS) analysis of the immunoprecipitated product identified an H2B protein (Figure 3A; Supplemental Data 1). Based on the results of Co-IP/MS and the fact that OsUBR7 contains a histone-recognizing PHD, we tested the physical interaction between OsUBR7 and four rice core histones (H3, H4, H2A, and H2B) through *in vitro* pull-down assays. Indeed, the GST-OsUBR7 fusion protein was precipitated with all the histone proteins but not with an MBP-only control (Figure 3B). Histone monoubiquitination predominately occurs on histones H2A and H2B (Joo et al., 2007; Weake and Workman, 2008; Richly et al., 2010). Therefore, we used bimolecular fluorescence complementation (BiFC) assays to validate the interaction between OsUBR7 and histone H2A or H2B. Co-expression of Vn-OsUBR7 and Vc-H2A or Vc-H2B reconstituted the GFP fluorescence, which was observed in the nuclei (Figure 3C).

Based on these results, we assumed that H2A and/or H2B might be the OsUBR7 substrates. The *in vitro* ubiquitination assay system is used to verify the function of putative E3 ligases, substrate ubiquitination, and E2 Ub conjugation (Zhao et al., 2013). Therefore, we used H2A or H2B as a substrate to determine the E3 ligase activity of OsUBR7 using a commercially available Ub kit. The results showed that OsUBR7 monoubiquitinated H2B but not H2A *in vitro*, and the human UbcH5b was the most suitable E2 conjugase for OsUBR7. In addition, we also found that the human UBR7-specific E2 conjugase UbcH6 could not conjugate with OsUBR7 (Figure 3D).

OsUBC18 serves as a specific E2 of OsUBR7 to mediate H2Bub1 at K148

There are 39 genes encoding E2 conjugases in rice (Bae and Kim, 2014; Zhiguo et al., 2015). We analyzed the sequence similarity of these rice E2 conjugases with human UbcH5b and found that OsUBC18 was the most likely ortholog of UbcH5b (Supplemental Figure 7). Indeed, OsUBC18 has very high amino acid sequence similarity to UbcH5b (Supplemental Figure 8A). Furthermore, OsUBC18 co-localized with OsUBR7 in the nuclei (Supplemental Figure 8B), suggesting that OsUBC18 may interact with OsUBR7 *in vivo*.

An E3 ligase must directly interact with a specific E2 conjugase to exert its enzymatic activity (Christensen et al., 2007; van Wijk et al., 2009; Bae and Kim, 2014; Polge et al., 2018). Indeed, we confirmed the physical interaction between OsUBR7 and OsUBC18 through an *in vitro* pull-down assay. His-tagged OsUBC18 precipitated with GST-OsUBR7 (Figure 4A), and a BiFC assay further validated the interaction between OsUBR7 and OsUBC18 in the nuclei by co-expression of Vn-OsUBR7 and OsUBC18-Vc (Figure 4B).

To further characterize the biochemical functions of OsUBR7 and OsUBC18, we expressed several recombinant proteins in *Escherichia coli*: E1 (His-AtUBA2), E2 (His-OsUBC18), E3 (His-OsUBR7), substrate protein (MBP-OsH2B.1), and Ub (His-AtUBQ14). We first determined the E2 Ub conjugation ability of OsUBC18 by a thioester assay and found that His-OsUBC18 bound Ub (Figure 4C). Then, we carried out *in vitro* ubiquitination assays and found that His-OsUBR7 monoubiquitinated MBP-OsH2B.1 *in vitro* with the help of His-OsUBC18 (Figure 4D).

To identify the monoubiquitination site on H2B, we compared the amino acid sequences of 10 rice H2B variants (Hu and Lai, 2015) and human H2B. Because human UBR7 monoubiquitinates human H2B at K120 (Adhikary et al., 2019), we selected K136, K144, and K148 as possible target lysine sites for OsUBR7 based on their alignment (Supplemental Figure 9). We then prepared native H2B (OsH2B.1) and mutant H2B proteins in which K136, K144, or K148 was replaced by arginine (R) (H2B_K136R, H2B_K144R, and H2B_K148R, respectively) as the substrates for an *in vitro* ubiquitination assay (Figure 4E). Only the K148R mutation resulted in complete loss of the modified MBP-H2bub1 band, indicating that the lysine site of the H2B variants corresponding to K148 of OsH2B.1 is the target for OsUBR7 (Figure 4F). We further examined the global H2Bub1 level in *osubr7* and WT plants using an anti-ubiquitinated histone H2B-specific antibody. The results showed that the global H2Bub1 level was significantly lower in the mutant (about half) than in WT plants (Figure 4G), further indicating that OsUBR7 acts as an H2BK148ub ligase *in vivo*.

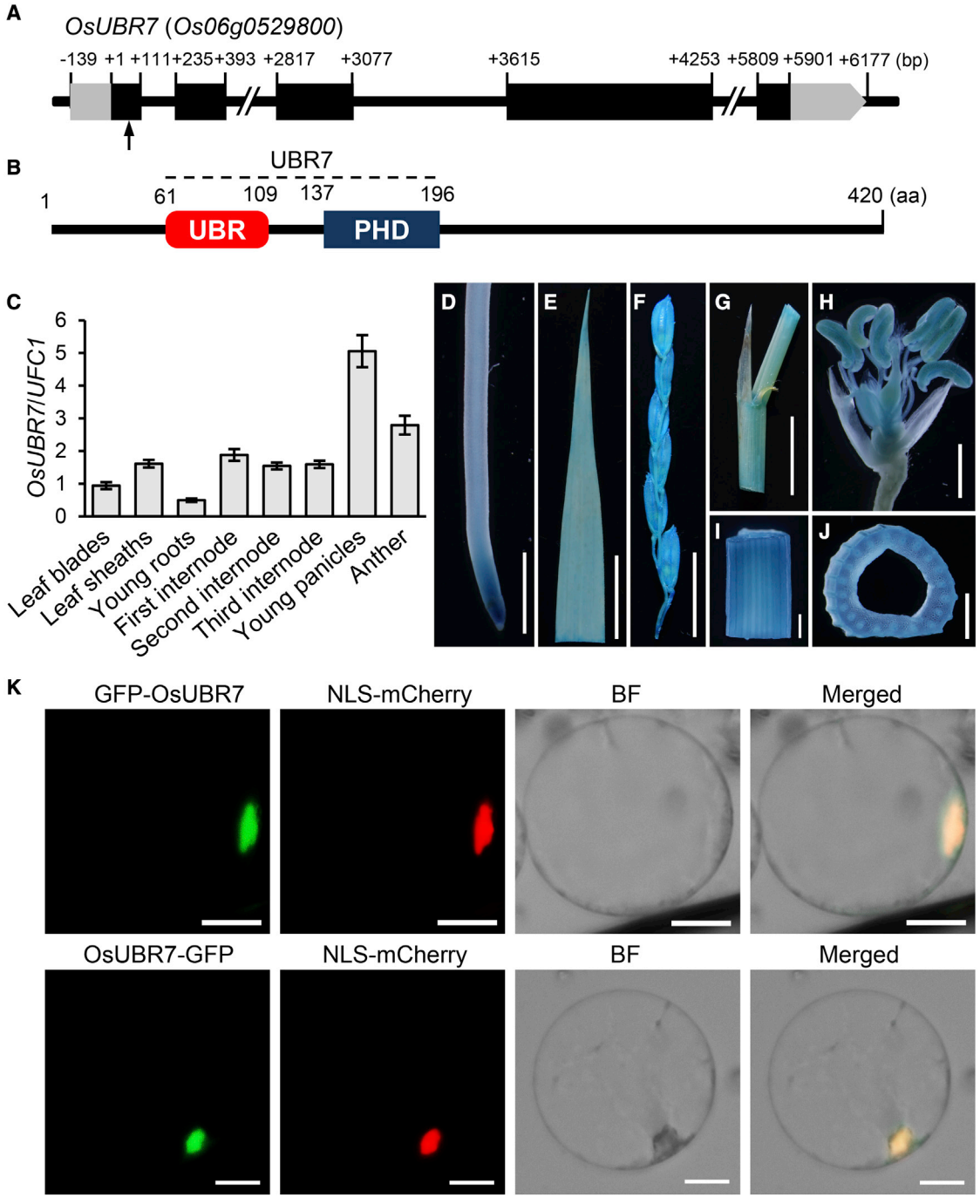

Figure 2. *OsUBR7* is constitutively expressed and encodes a nucleus-localized UBR7 protein.

(A) Schematic of the *OsUBR7* gene structure. The arrow shows the target site for CRISPR–Cas9 editing.

(B) Diagram of the conserved domains in OsUBR7. UBR, Ub ligase N-recognin box; PHD, plant homeodomain finger; UBR7, ubiquitin protein ligase E3 component N-recognin 7.

(C) Relative *OsUBR7* expression in different tissues. The levels of *OsUBR7* transcripts were normalized to those of *UFC1*. Data are means ± SD (n = 3 biological repeats).

(D–J) Histochemical staining analysis of expression of the *OsUBR7-GUS* fusion transgene (driven by the native *OsUBR7* promoter) in various tissues of transgenic plants. GUS signals were detected in the root tip **(D)**, leaf **(E)**, spikelets **(F)**, leaf blade and sheath **(G)**, pistils and stamen **(H)**, and stem section **(I and J)**. Scale bars in **(E)**, **(F)**, and **(G)**, 1 cm. Scale bars in **(D)**, **(H)**, **(I)**, and **(J)**, 1 mm.

(K) Subcellular localization of OsUBR7-GFP and GFP-OsUBR7 fusion proteins in rice sheath protoplasts. The NLS-mCherry fusion protein served as a nuclear marker. BF, bright field image. Scale bars, 10 μm.

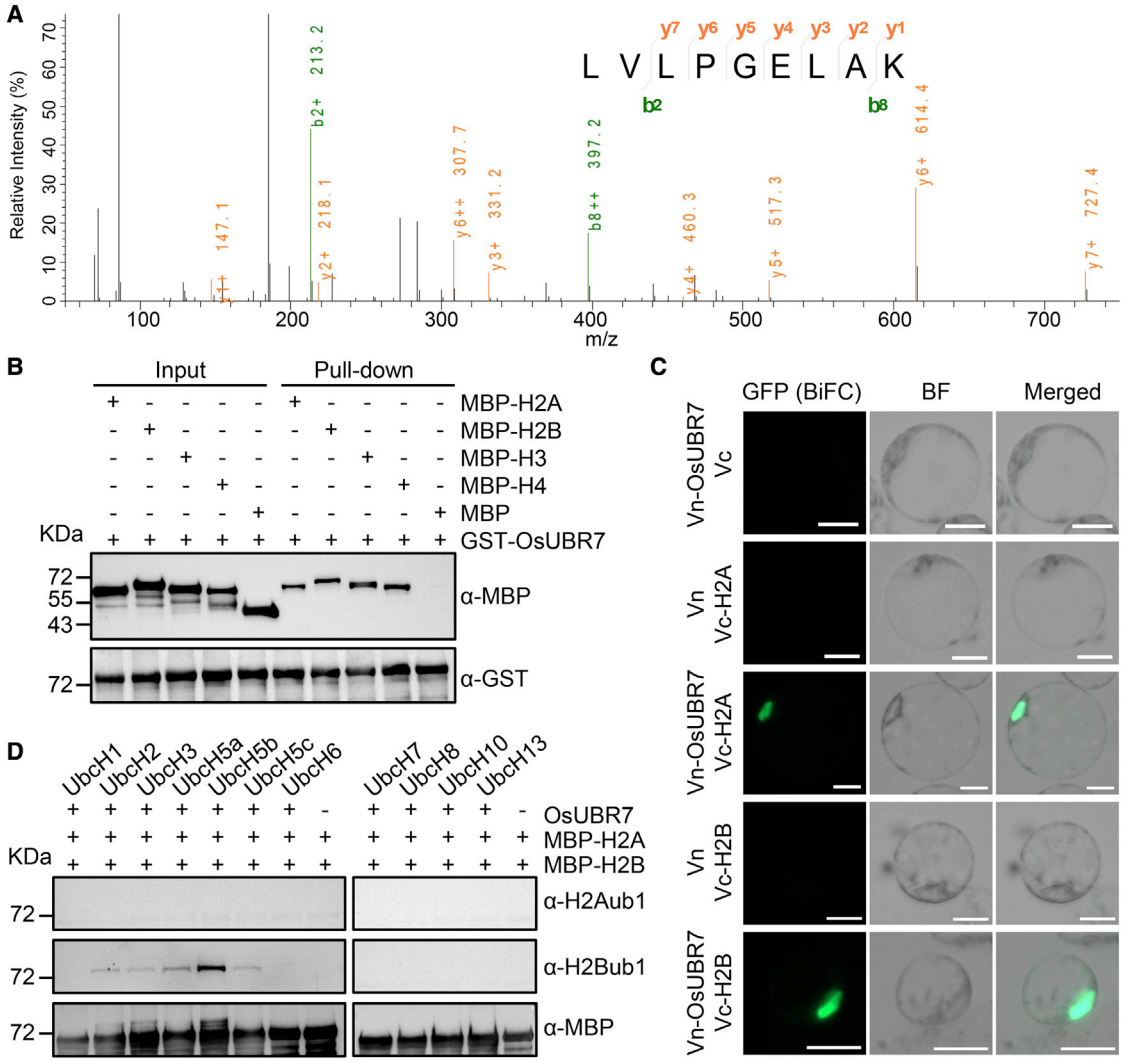

Figure 3. H2B is a substrate for OsUBR7-mediated monoubiquitination.

(A) OsUBR7 interacted with H2B. Total proteins were extracted from transgenic *OsUBR7-FLAG* overexpression rice plants and immunoprecipitated for mass spectrometry. The LVLPGELAK peptide of H2B was identified in the OsUBR7-FLAG-immunoprecipitated complex.

(B) *In vitro* GST pull-down assay to examine the interactions between OsUBR7 and multiple histone proteins. OsUBR7 was fused with GST, and H2A, H2B, H3, and H4 were fused with MBP; MBP served as a control. The presence (+) and absence (−) of components in the reaction mixture are indicated. The precipitated multiple histone proteins associated with the immobilized GST-OsUBR7 were detected by western blotting with anti-MBP or anti-GST antibodies.

(C) BiFC assays in rice sheath protoplasts demonstrating the interaction of OsUBR7 with H2A and H2B. Vn- and Vc- refer to the fused proteins with the N or C terminus of GFP, respectively, in the BiFC assay. The merged image includes combined images from the GFP and differential interference contrast channels. Scale bars, 10 μm.

(D) *In vitro* ubiquitination assay using recombinant MBP-H2A and MBP-H2B as substrates to identify the corresponding E2s (UbcHs) for OsUBR7; UbcH5b showed the strongest monoubiquitination signal for H2B.

OsUBR7 mediates H2Bub1 to regulate expression of target genes and cell proliferation

Previous studies have revealed that human H2BK121ub1 and the associated methylation of histone H3K79 affect expression of target genes (Briggs et al., 2002; Wojcik et al., 2018; Worden et al., 2019). Thus, we proposed that OsUBR7 may play important roles in transcriptional activation. To find genes that are transcriptionally activated by OsUBR7-mediated histone modification, we performed chromatin immunoprecipitation (using anti-H2Bub1 antibody) followed by sequencing (ChIP-seq) and transcriptome sequencing using WT and *osubr7* seedlings. The ChIP-seq results showed that the number (1654) of gene loci with downregulated H2Bub1 levels (a total of 1695 peaks) in *osubr7* versus WT was much greater than that of loci with upregulated H2Bub1 levels (253 peaks), and these differential H2Bub1 peaks were distributed across the genome (Supplemental Figure 10A; Supplemental Data 2). Several representative examples of gene loci with obviously reduced H2Bub1 levels in *osubr7* are shown (Figure 5A; Supplemental Figures 11A and 11B). We then selected two pleiotropic genes and two cell-cycle-related genes for ChIP–qPCR validation, which confirmed that the H2Bub1 levels of these gene loci were decreased (Figure 5B).

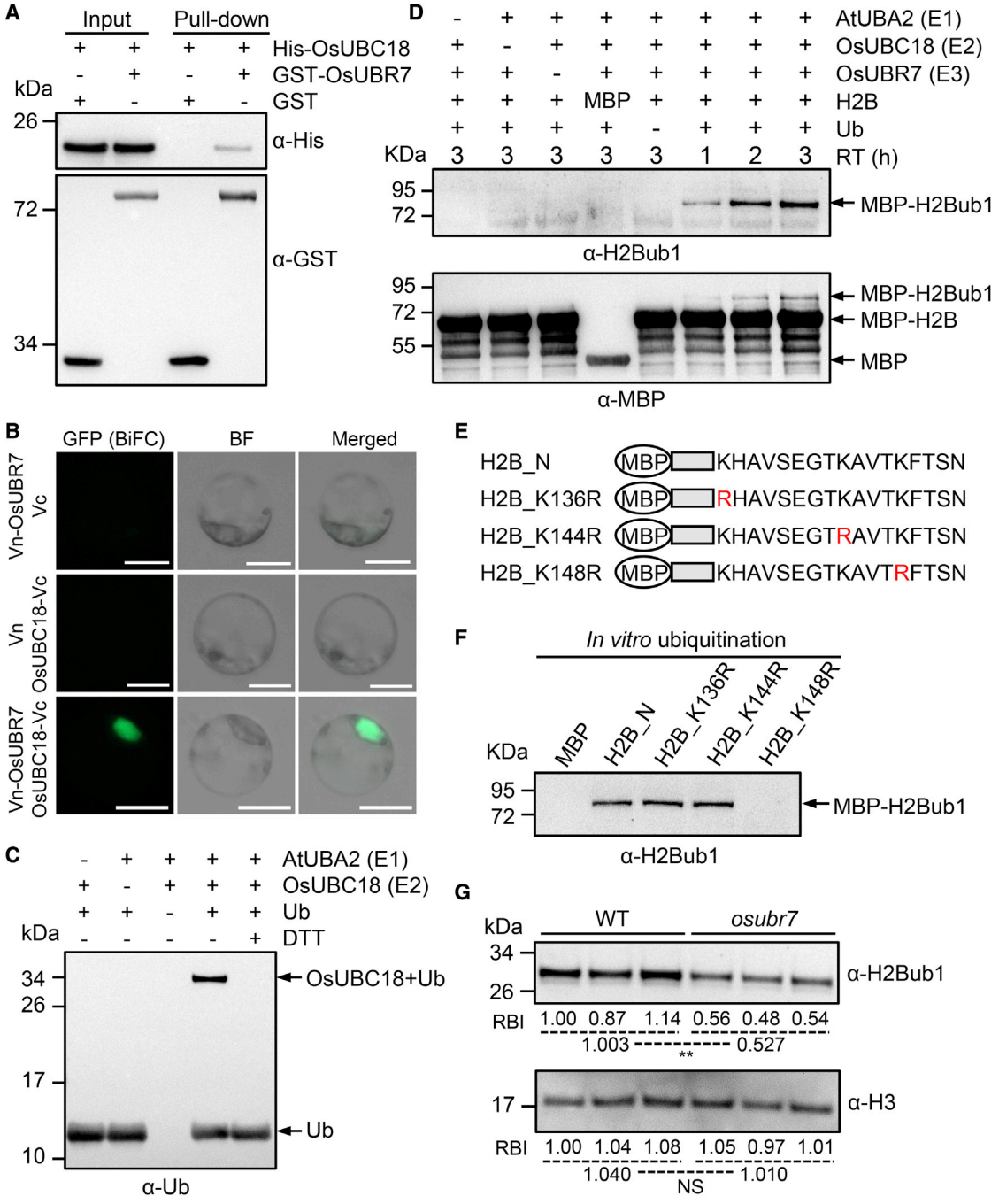

Figure 4. OsUBR7 monoubiquitinates H2B at K148, and OsUBC18 serves as its specific E2.

(A) *In vitro* GST pull-down assay to examine the interaction between OsUBR7 and OsUBC18. OsUBR7 was fused with GST, OsUBC18 was fused with His, and GST served as a control. Precipitated His-OsUBC18 associated with immobilized GST-OsUBR7 was detected by western blotting with anti-His or anti-GST antibody.

(B) BiFC assays in rice sheath protoplasts demonstrating that OsUBR7 interacted with OsUBC18. Scale bars, 10 μm.

(C) Thioester assay for the activity of recombinant His-OsUBC18. Binding of OsUBC18 with Ub was detected with anti-Ub antibody. Thioester binding was disrupted in the presence of the reducing agent DTT.

(D) *In vitro* ubiquitination assay using recombinant His-AtUBA2 as E1, His-OsUBC18 as E2, His-OsUBR7 as E3, and MBP-H2B as substrate. Ubiquitinated MBP-H2B was detected with anti-H2Bub1 or anti-MBP antibody. RT, reaction time (h).

(legend continued on next page)

These results indicate that OsUBR7 indeed performs H2B mono-ubiquitination at certain chromatin sites.

By combining the ChIP-seq and transcriptome sequencing data (Supplemental Data 3), we selected 119 overlapping genes with downregulated H2Bub1 and expression levels in *osubr7* versus WT seedlings (Supplemental Figure 10B; Supplemental Data 4), which may be target genes regulated directly by OsUBR7. Several of these genes are responsible for pleiotropic phenotypes in rice, such as *OsGS2*, which regulates plant height, tiller number, and grain weight (Cai et al., 2010), *OsTrxm*, which affects plant height and leaf color (Chi et al., 2008), and *FLO2*, which controls grain size (She et al., 2010). We then selected five of these genes for qRT–PCR analysis and confirmed their reduced expression in *osubr7* (Figure 5C).

Gene Ontology (GO) analysis of the H2Bub1-downregulated genes in *osubr7* compared with WT showed that the functional categories "positive regulation of G2/M transition of mitotic cell cycle" and "mitotic cell cycle" were significantly enriched (Supplemental Figure 12). Cell-cycle-related proteins are mainly responsible for DNA synthesis, which is the main cellular activity in the S phase of the cell cycle (Siqueira et al., 2018; Liu et al., 2019). In line with the significantly lower global H2Bub1 level in *osubr7* plants, numerous cell-cycle-related genes may be downregulated in the mutant. As expected, the expression levels of 19 cell-cycle-related genes, including the cell-cycle marker genes *CDKB;1*, *CDKB2;1*, *CDKD;1*, *CYCA2;1*, *CYCA3;2*, and *H4* (Yuan et al., 2010; Niu et al., 2017), were significantly downregulated in *osubr7* (Figure 5D; Supplemental Figure 13).

The involvement of OsUBR7 in the transcriptional activation of cell-cycle-related genes could explain the significant reduction in cell number observed in *osubr7* internodes and glumes. We next performed flow cytometry assays to analyze cell-cycle progression in 7-day-old *osubr7* and WT seedlings. Compared with the WT, *osubr7 seedlings* had a significantly higher proportion of nuclei with 4C DNA content (Figure 5E) and significantly more cells at the S and G2/M phases of the cell cycle (about 23.51% versus about 17.13% in the WT; Figure 5F), suggesting that cell-cycle progression was suppressed in the mutant.

OsUBR7 divergence may have undergone selection during rice domestication

To characterize the genetic diversity of *OsUBR7*, we investigated haplotype variation at this locus based on a public genome database for the *Oryza* species (Kajiya-Kanegae et al., 2021). In 1491 *japonica*, 3019 *indica*, and 98 wild rice (*O. rufipogon*, *O. barthii*, *O. longistaminata*, *O. minuta*, and *O. brachyantha*) accessions, a total of 23 single-nucleotide polymorphisms (SNPs) were detected in the *OsUBR7* coding region, and 24 haplotypes (cH1–cH24) were classified (Supplemental Figure 14; Supplemental Data 5). In the *OsUBR7* promoter region (from −18 to −804 bp) of these rice accessions, there were 45 SNPs (including some base deletions in a few accessions), and they were grouped into 41 promoter haplotypes (pH1–pH41) (Supplemental Figure 15). Analysis of the dominant haplotypes (cH1–cH4, pH1–pH5) in cultivated rice showed that they are strongly associated with the *japonica* or *indica* accessions. For example, cH1 and pH1 are mainly present in the *japonica* accessions (79.3% of *japonica* and 1.6% of *indica* accessions contain cH1, i.e., a rate 0.98 of cH1 presenting in *japonica*; 79.7% of *japonica* and 1.6% of *indica* accessions contain pH1, i.e., a rate 0.98 of pH1 presenting in *japonica*) (Figure 6A). By contrast, cH2, pH2, and pH3 are the major haplotypes of the *indica* accessions (84% of *indica* and 4.4% of *japonica* accessions contain cH2, i.e., a rate 0.95 of cH2 presenting in *indica*; 78.5% of *indica* and 2.2% of *japonica* accessions contain pH2 or pH3, i.e., a rate 0.97 or 0.98 of pH2 or pH3 presenting in *indica*) (Figure 6A). Notably, the dominant haplotypes cH1 and pH1–pH5 in cultivated rice were not detected in the wild rice species, whereas cultivated rice contained only a small fraction of the haplotypes present in *O. rufipogon* (Supplemental Figures 14 and 15). This result suggests that these major haplotype variations occurred during the domestication of the rice subspecies and were selected, especially in *japonica* populations.

We further analyzed population differentiation (F_{ST}) and pooled heterozygosity (H_p) at and around the *OsUBR7* locus. The results showed that the F_{ST} sweep around the *OsUBR7*-containing regions had scores near 0.6, and the F_{ST} values of a number of SNPs at the *OsUBR7* locus were greater than 0.8 or 0.9 (Figure 6B), which can be considered as significant differentiating and fixing sites (Frankham et al., 2002). Correspondingly, the *japonica* and *indica* H_p scores of these SNPs with high F_{ST} values at *OsUBR7* were reduced to zero or nearly zero (Figure 6B), indicative of selection during evolution. These results suggest that the genetically divergent *OsUBR7* alleles have undergone natural and artificial selection during domestication of the cultivated rice subspecies, leading to high degrees of fixation (i.e. high F_{ST} values).

To determine whether haplotype variations of the *OsUBR7* alleles between *japonica* and *indica* cultivar groups affect expression activity, we analyzed four *japonica* cultivars (with pH1/cH1 or pH1/cH2) and four *indica* cultivars (with pH3/cH2 or pH8/cH2) by qRT–PCR. The results showed that the *japonica* cultivars had significantly higher expression levels of *OsUBR7* than the *indica* cultivars (Figure 6C). It is notable that the haplotypes pH2–pH4 and pH6–pH13 detected in a majority of *indica* accessions carried three common SNPs (sites 27, 28, and 41; Supplemental Figure 15), which may be involved in the decreased transcription activity of the *OsUBR7* alleles in the *indica* cultivars. These observations suggest possible

(E) Schematic of the C-terminal region of the MBP-tagged H2B (OsH2B.1) native construct (H2B_N) and its mutant forms, in which K136, K144, or K148 was replaced by R (H2B_K136R, H2B_K144R, and H2B_ K148R, respectively).

(F) *In vitro* ubiquitination assay using the H2B native construct (H2B_N) or a mutant variant (H2B_K136R, H2B_K144R, or H2B_K148R) as a substrate. Ubiquitinated MBP-H2B was detected with the anti-H2Bub1 antibody.

(G) Comparison of H2Bub1 levels between WT and *osubr7* plants by western blotting. H3 protein was detected as a loading control. Values of relative band intensity (RBI) to the first lanes from the left are given below the bands. $^{**}p < 0.01$ (Student's *t*-test). NS, not significant.

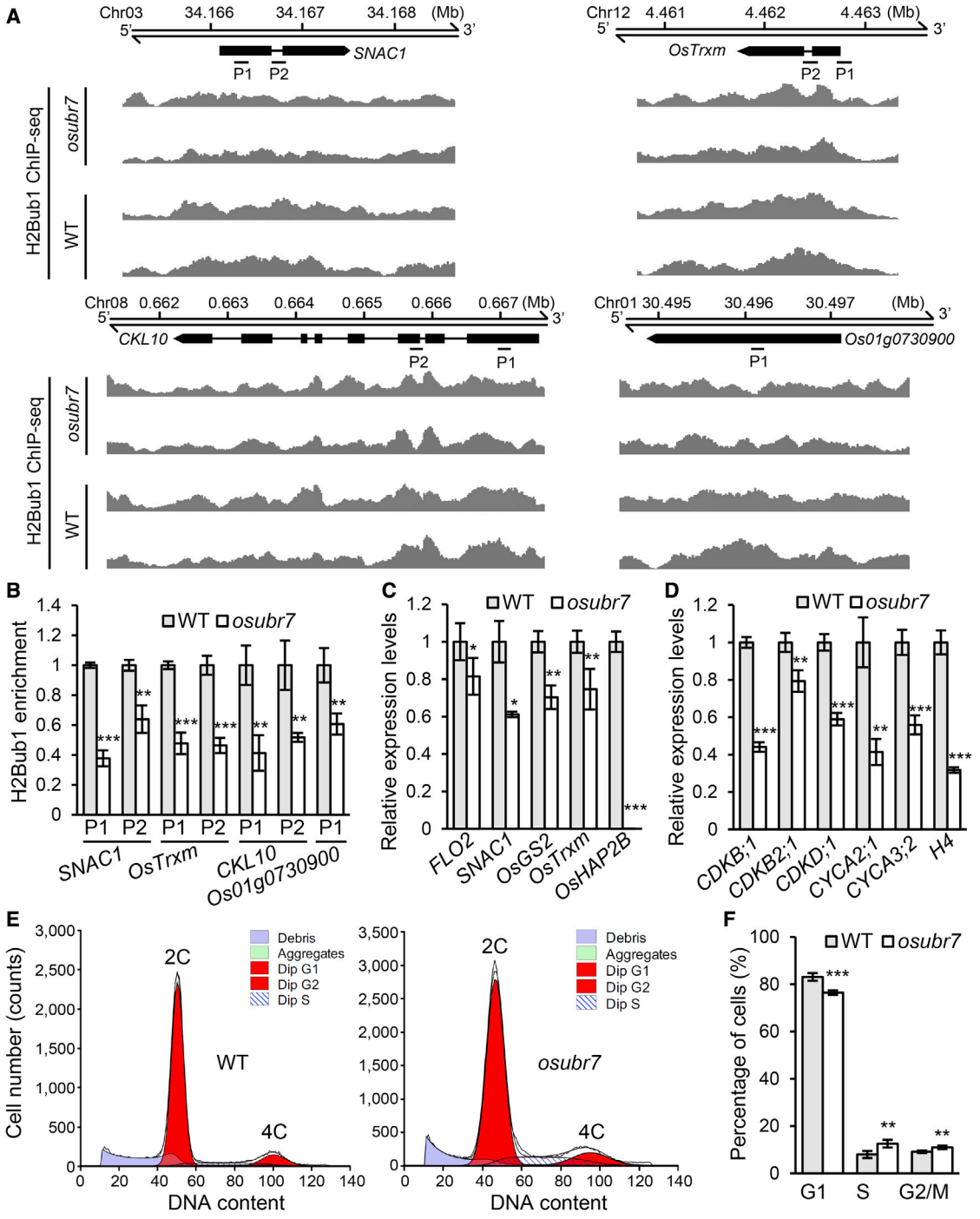

Figure 5. Downregulated expression of target genes by OsUBR7-mediated reduction of H2Bub1 results in suppression of cell-cycle progression.

(A) Diagrammatic representation of ChIP-seq maps (using an anti-H2Bub1 antibody; $n = 2$ biological repeats) for four gene loci at which the H2Bub1 level was completely suppressed or decreased in *osubr7 seedlings*.

(B) ChIP–qPCR analysis to determine H2Bub1 levels in candidate target genes, including the two pleiotropic genes and two cell-cycle-related genes shown in **(A)**. P1 to P2 represent regions covered by the primers used to assess the level of H2Bub1 by qPCR following ChIP. Data were normalized to the input chromatin, *OsNRAMP2* was used as the reference, and the values of H2Bub1 levels in the WT were set to 1. Values are means ± SD ($n = 3$ biological repeats). $^{**}p < 0.01$ and $^{***}p < 0.001$ (Student's *t*-test).

(C) qRT–PCR analysis of five pleiotropic genes selected from the ChIP-seq and transcriptome data in 14-day-old WT and *osubr7* seedlings. *Actin1* was used as the reference, and the values of expression levels in the WT were set to 1. Values are means ± SD ($n = 3$ biological repeats). $^{*}p < 0.05$, $^{**}p < 0.01$, and $^{***}p < 0.001$ (Student's *t*-test).

(legend continued on next page)

correlations among genetic diversity, functional activity, and organ development in the rice subspecies.

To further analyze whether the different *OsUBR7* haplotypes affect plant height, we used plant height data of 527 rice accessions from RiceVarMap2 to perform specific association analysis of the dominant haplotypes (cH1–cH5 and pH1–pH5) with plant height. We found that the *OsUBR7* haplotypes cH3, cH5, and pH4 were significantly associated with plant height (Supplemental Figures 16A and 16B).

Potential utility of *OsUBR7* for regulating plant height during breeding

Elite semi-dwarf rice varieties usually have ideal plant heights ranging from about 90 to 115 cm. To test whether mutant alleles of *OsUBR7* could be used to improve the plant height of rice, we knocked out *OsUBR7* in the *japonica* cultivar Taichung 65 (T65) that has a taller plant height (about 120 cm) and lower tiller numbers. The *osubr7-T65* mutant lines showed a better plant type than WT T65, with heights of 90–95 cm (Supplemental Figures 17A and 17B). Although the grain weight was slightly reduced in these lines, their grain yield per plant was not significantly different from that of the WT owing to increased tiller (panicle) number per plant (Supplemental Figures 17C–17H), highlighting the potential for using mutant alleles of *OsUBR7* in rice breeding.

DISCUSSION

In this study, we demonstrate that OsUBR7 acts as an epigenetic regulator of many gene loci related to cell proliferation and organ development. OsUBR7 functions as a new E3 ligase for H2B monoubiquitination in rice. In WT plants, OsUBR7 specifically binds to H2B of certain chromatin regions and monoubiquitinates the H2B tail at K148, and OsUBC18 acts as its specific E2. This E1-OsUBC18-OsUBR7 H2Bub1 pathway, possibly together with the E1-E2-OsHUB1/2 H2Bub1 pathway, dynamically regulates H2Bub1 levels at target gene loci, including a number of cell-cycle-related genes and pleiotropic trait genes. These chromatin states of the gene loci enable their normal transcription and cell-cycle progression to ensure development (Figure 7A). Loss of function of OsUBR7 results in decreased H2Bub1 and expression levels of the target genes. The suppression of cell-cycle progression produces shorter internodes (and thus semi-dwarf stature) and other trait variations (Figure 7B).

Among the seven UBR box-containing protein groups (UBR1–UBR7), the UBR7 group is less studied, and their biochemical functions in plants have not been tested (Tasaki et al., 2005, 2012; Tasaki and Kwon, 2007; Sriram et al., 2011; Zhang et al., 2019). Human UBR7 binds to soluble histone H3 via its PHD (Kleiner et al., 2018). The PHD is commonly recognized as a conserved histone recognition element and is often present in chromatin-modifying enzymes (Kleiner et al., 2018; Adhikary et al., 2019; Longbotham et al., 2019). In fact, our experiments demonstrated that OsUBR7 is located in nuclei and interacts with all the histones, possibly through its PHD. UBR7 proteins are widely present in eukaryotes but not in prokaryotes. Another plant UBR7 protein, NbUBR7 of *Nicotiana benthamiana*, has a very different function from human UBR7. NbUBR7 interacts with the Toll-interleukin-1-receptor (TIR) homology domain present in some nucleotide-binding leucine-rich repeat (NLR) immune receptors, termed TIR-NLRs, to regulate NLR immune-receptor-mediated immunity (Zhang et al., 2019). However, TIR-NLRs are present only in dicotyledonous plants, and rice lacks TIR-NLRs entirely (Caplan et al., 2008; Cesari et al., 2014; Cui et al., 2015; Ve et al., 2015). This shows that rice UBR7 has a different function from NbUBR7. In addition, our test found that human UbcH5b could serve as an E2 conjugase of OsUBR7 *in vitro*, and OsUBC18 is the ortholog of UbcH5b. However, the E2 conjugase of human UBR7 is UbcH6 rather than UbcH5b; in rice, there is no ortholog of UbcH6. This result suggests the evolved specificity of UBR7-based H2Bub1 systems between plants and humans.

Previous studies have shown that the plant RING finger-E3 ligases (rice OsHUB1 and OsHUB2, *Arabidopsis* AtHUB1 and AtHUB2, and tomato SlHUB1 and SlHUB2) are also H2Bub1 ligases that play important roles in chromatin epigenetic regulation, affecting growth and development as well as stress response (Fuchs et al., 2012; Zhang et al., 2015; Zhao et al., 2019). Our study demonstrates that plant UBR7 finger-E3 ligases, such as OsUBR7 analyzed in this study, represent a novel chromatin H2Bub1 mechanism; the combination of the HUB1/2 and UBR7 pathways constitutes a complete H2Bub1 system in plants, extending the H2Bub function of the UBR7 family to plants.

Genetic variations in gene loci that control agronomic traits are the main targets used for plant breeding. However, increasing evidence suggests that epigenetic and epigenomic regulation processes such as chromatin remodeling also have great potential to contribute to trait variations in plant species and are thus important epigenetic resources for improvement of agronomic traits (Springer and Schmitz, 2017). In cereal crops, semi-dwarf stature is a valuable agronomic trait that can increase lodging resistance, harvest index, and grain yield (Ferrero-Serrano et al., 2019). Semi-dwarf breeding in wheat (*Triticum aestivum*) and rice has increased global grain production since the 1960s. However, semi-dwarf rice breeding programs are mostly dependent on the utilization of *sd1* alleles (Gaur et al., 2020). Therefore, the discovery of new semi-dwarf germplasm resources will extend genetic and epigenetic diversity and increase yield potential in crop breeding (Spielmeyer et al., 2002; Hedden, 2003; Wang et al., 2005; Liu et al., 2018).

In this study, we demonstrate that the *OsUBR7* locus region is highly polymorphic and that the divergent *OsUBR7* alleles may

(D) Relative expression of six cell-cycle marker genes in 14-day-old WT and *osubr7* seedlings. *UFC1* was used as the reference, and the values of expression levels in the WT were set to 1. Values are means ± SD (n = 3 biological repeats). $^{**}p < 0.01$ and $^{***}p < 0.001$ (Student's t-test). NS, not significant.

(E) Cell numbers during cell-cycle phases with 2C and 4C nuclei in WT and *osubr7* seedlings (7 days old) measured by flow cytometry.

(F) Percentage of cells in different phases of the cell cycle in WT and *osubr7* seedlings. Data are means ± SD (n = 4 biological repeats). $^{**}p < 0.01$ and $^{***}p < 0.001$ (Student's t-test).

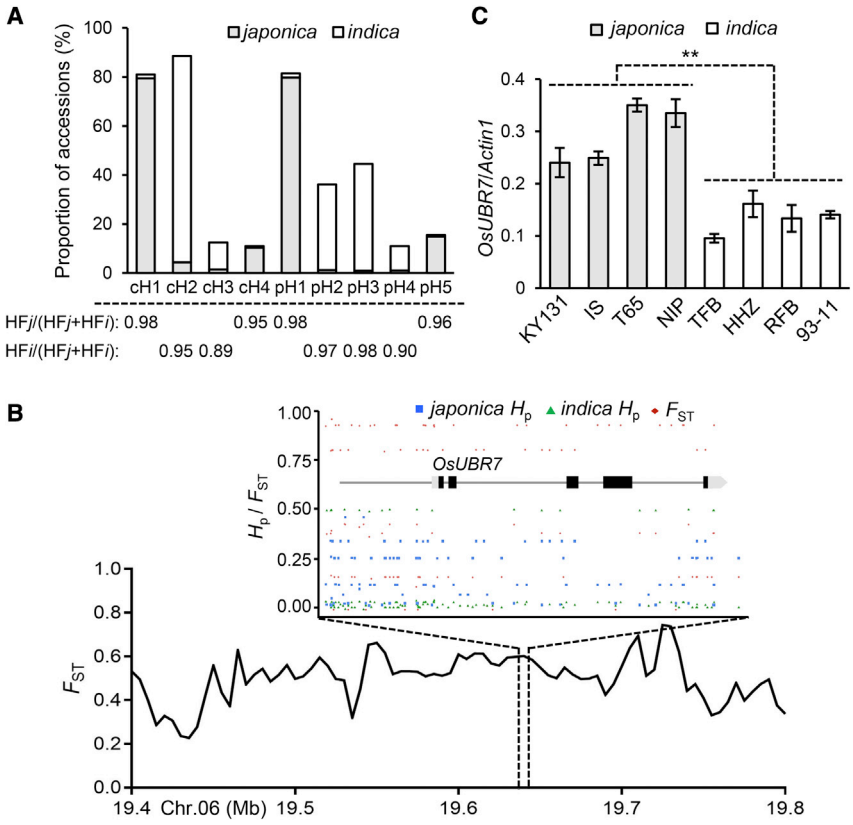

Figure 6. Distribution of major haplotypes of the *OsUBR7* locus and their selection during rice domestication.

(A) Frequencies of major haplotypes in 1491 *japonica* and 3019 *indica* cultivars, and rates of haplotype frequencies in the *japonica* group (HF*j*) or *indica* group (HF*i*).

(B) Population difference (F_{ST}) and pooled heterozygosity (H_p) analyses of SNP sites around and at the *OsUBR7* locus in 1491 *japonica* and 3019 *indica* cultivars. The F_{ST} sweep on the chromosomal region was performed using a 10-kb scanning window with a 5-kb step. The F_{ST} and H_p scores at the *OsUBR7* locus were estimated based on individual SNPs.

(C) The expression levels of *OsUBR7* differed significantly between *japonica* and *indica* groups. The tested *japonica* cultivars KY131, Ishikari Shiroke (IS), and Nipponbare (NIP) had haplotypes pH1/cH1, and Taichung 65 (T65) contained pH1/cH2; the *indica* cultivars carried pH3/cH2 (for 93-11) or pH8/cH2 (for TFB, HHZ, and RFB), as shown in Supplemental Figures 14 and 15. Note that pH3 and pH8 had three common SNPs (sites 27, 28, and 41). Data are means ± SD (n = 3 biological repeats). $^{**}p < 0.01$, significant difference in expression levels (by qRT–PCR) between the *japonica* and *indica* cultivar groups.

have undergone selection during evolution and contributed to the domestication of the *japonica* and *indica* subspecies. Indeed, the divergent *OsUBR7* alleles (different haplotypes) in *japonica* and *indica* cultivars showed varied transcriptional activities (Figure 6C), and some were associated with plant height (Supplemental Figures 16A and 16B). This genetic divergence may have some impact on the fitness and/or development of the subspecies. Our primary test of editing *OsUBR7* in the taller rice cultivar T65 showed that the mutant plants exhibited a better plant type without obvious reduction in grain yield, suggesting a potential strategy for rice improvement. Plant type and other rice agronomic traits could also be improved by fine-tuning *OsUBR7* expression pattern and/or level, rather than by complete function knockout of *OsUBR7*. This could be achieved by editing *cis* regulatory elements in its promoter/UTR/intron regions, thus avoiding possible negative effects of complete knockout. In addition, considering the functional conservation of *UBR7* genes in plants, this study provides a possible new target for improving agronomic traits in other crops.

METHODS

Plant materials

The *osubr7* mutant was identified in a mutant library of the *japonica* cultivar Nipponbare. The highly specific target site for CRISPR–Cas9 editing in the first exon of *Os06g0529800* was designed using the web-based tool CRISPR-GE (Xie et al., 2017). The CRISPR–Cas9 binary construct was constructed according to Ma et al. (2015). The entire 9385-bp genomic sequence of *Os06g0529800* was isolated by PCR and inserted into the binary vector pCAMBIA1300 by Gibson Assembly (Gibson, 2011) to generate the complementation construct. Another binary overexpression construct containing full-length *Os06g0529800* cDNA fused with the 3x FLAG sequence driven by the maize (*Zea mays*) *Ubiquitin* promoter was generated using a PCR-based strategy and inserted into the binary vector pCAMBIA1300. All constructs were transformed into Nipponbare (for CRISPR–Cas9 mutagenesis) or the *osubr7* mutant (for transgenic complementation) by *Agrobacterium tumefaciens*-mediated transformation. More than 10 independent transgenic lines were generated from each transformation. The DSDecode program was used to analyze the mutation sites (Liu et al., 2015). OsUBR7-FLAG protein in transgenic overexpression lines was analyzed using western blotting with antibodies against FLAG (mouse, Sigma F1804, 1:2000 dilution). The plant materials were grown in paddy fields or greenhouses of South China Agricultural University, Guangzhou. All primers used in this study (including those described below) are listed in Supplemental Data 6.

Measurement of agronomic traits

Agronomic traits including plant height, internode length, panicle morphology, and grain number were measured on the main culm. Tiller number was measured for whole plants. Dried grains were used to measure grain length, width, and weight. Seedling height was measured in 3-week-old rice plants. Traits of *osubr7* plants (in the Nipponbare background) were measured in the T_4 generation. Traits of *OsUBR7*-complementation and -overexpression lines were measured in the T_2 generation. Traits of *osubr7*-knockout lines in the T65 background were measured in the T_3 generation.

Tissue sectioning and GUS staining

Fresh second internodes were cut into ~0.5 cm lengths, fixed with Carnoy's fluid, and placed under vacuum to allow the fixative to penetrate the tissue. The internodes were fixed overnight and dehydrated with a graded ethanol series and a graded xylene series. The internodes were embedded in paraffin (Sigma, Burlington, MA, USA), cut into 10-mm sections, and mounted on glass slides using poly-D-lysine (Sigma). The

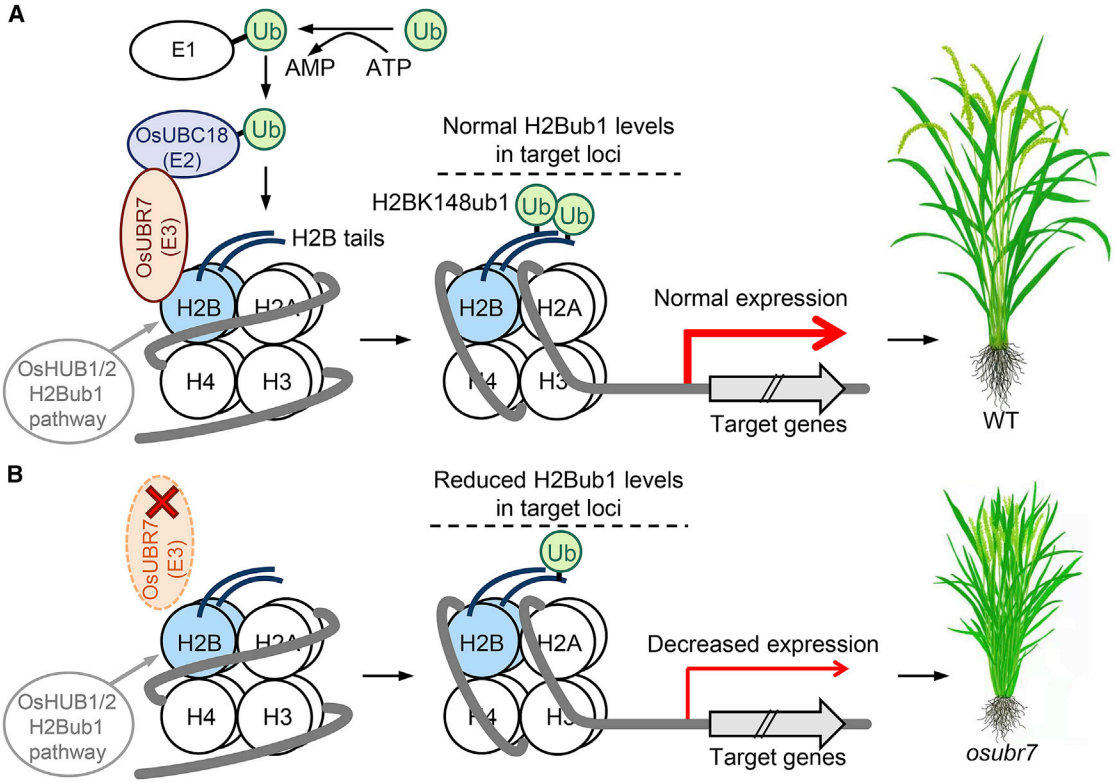

Figure 7. A working model for the molecular function of OsUBR7 in rice development.

(A) In WT plants, OsUBR7 functions as an E3 ligase. It binds to an E2 conjugase (OsUBC18) and a substrate (H2B) in the target chromatin regions and transfers ubiquitin from OsUBC18 to K148 of H2B. This E1-OsUBC18-OsUBR7 H2Bub1 pathway, possibly together with the E1-E2-OsHUB1/2 H2Bub1 pathway, results in normal H2Bub1 levels at target gene loci (including cell-cycle-related and pleiotropic genes) for their normal transcription, ultimately properly controlling cell-cycle progression and normal organ development.

(B) In *osubr7* plants, the lack of OsUBR7 results in reduced H2Bub1 levels (basal H2Bub1 levels may depend on the OsHUB1/2-mediated pathway) and decreased expression of the target genes. The suppressed cell-cycle progression leads to semi-dwarfing and other trait variations of *osubr7* plants.

prepared sections were baked in a 40°C oven overnight and then stained in 1% toluidine blue solution for 15 min. The sections were then dewaxed twice in xylene and sealed with coverslips after adding neutral resin. Slides were observed with a microscope (Carl Zeiss, Jena, Germany) and photographed.

The GUS assay was performed using a commercial GUS staining buffer following the manufacturer's instructions (Real-Times [Beijing] Biotechnology, Beijing, China). In brief, different tissues from *Pro-gOsUBR7-GUS* transgenic plants were incubated in GUS staining buffer at room temperature overnight in the dark and then washed with 70% ethanol. The GUS-stained tissues were further imaged using a zoom stereo microscope (Olympus, Tokyo, Japan).

Scanning electron microscopy

Mature grains were dried in a critical point drier and coated with gold sputter. For epidermal cell observation, the outer surfaces of the whole lemmas were observed with a scanning electron microscope (Carl Zeiss). Cell size and cell number were calculated along the longitudinal axis.

RT and qRT–PCR analysis

For gene expression analysis, total RNA was isolated from rice leaves, sheaths, roots, internodes, panicles, and anthers with TRIzol reagent (Thermo Fisher Scientific, Waltham, MA, USA) according to the manufacturer's instructions. cDNA was synthesized from total RNA using M-MLV Reverse Transcriptase (Promega, Madison, WI, USA) according to the manufacturer's instructions. qRT–PCR was performed using the CFX96 Real-Time PCR System (Bio-Rad, Hercules, CA, USA) with three biological repeats. Rice *HOMOLOG OF UFM1-CONJUGATING ENZYME 1* (*UFC1*) was used as an internal control to normalize the expression of target genes (Zhao et al., 2020). Relative expression levels were measured using the $2^{-\Delta\Delta Ct}$ method.

Subcellular localization and BiFC assays

The full-length coding sequence of *OsUBR7* was cloned into vectors pD1-N-GFP and pD1-C-GFP (Han et al., 2022). The nuclear marker construct NLS-mCherry was transiently co-expressed in rice leaf sheath protoplasts with the polyethylene glycol–calcium method (Chen et al., 2006, 2010). For the BiFC assay, the pVN and pVC vectors were fused with the N or C terminus of GFP. The different protein combinations were visualized by confocal microscopy (Carl Zeiss).

Bioinformatics analysis

The NCBI CDD (https://www.ncbi.nlm.nih.gov/Structure/bwrpsb/bwrpsb.cgi) and SMART database (http://smart.embl-heidelberg.de/) were used to confirm the conserved domains of OsUBR7. Amino acid sequences of UBR7 proteins, as well as rice E2 conjugases and human UbcH5b, were aligned using MEGA-X software with the ClustalW algorithm and gap-open and gap-extension penalties of 10 and 0.2, respectively. Aligned sequences were used to construct an unrooted phylogenetic tree based on the neighbor-joining method after bootstrap analysis for 10 000 replicates. The conserved domains of UBR7 in a variety of eukaryotes were analyzed using NCBI CDD and visualized using TBtools

software (v.1.098689) (Chen et al., 2020). Clustal Omega online software (https://www.uniprot.org/align/) was used to analyze the amino acid sequence conservation of OsUBC18 and UbcH5b, as well as 10 rice H2B variants and human H2B.

Co-IP/MS assay

To identify OsUBR7-interacting proteins, total proteins were extracted from 2-week-old WT and *OsUBR7-FLAG* overexpression seedlings (*OsUBR7*^{OE}#9) using plant cell lysis buffer (catalog number [Cat#]: P0043, Beyotime Biotechnology, Shanghai, China). Next, anti-FLAG affinity gel (Cat#: 20585ES01, Yeasen Biotechnology, Shanghai, China) was added to the lysis buffer, followed by incubation overnight. The affinity gels were washed three times with lysis buffer, and elution buffer was added to release the proteins. The eluted proteins were reduced with Tris (2-carboxyethyl) phosphine at 60°C for 1 h, then methyl methanethiosulfonate was added and incubated for 45 min in the dark. The protein solution was transferred to a 10-kDa ultrafiltration tube (PALL, Port Washington, NY, USA) and centrifuged at 12 000 × *g* for 20 min. Urea solution (8 M urea, pH 8.5) was added, and the mixture was centrifuged twice under the same conditions. Finally, 0.25 M tetraethylammonium bromide solution was added and centrifuged three times under the same conditions. The centrifuged supernatants were further digested with trypsin (Cat#: V5280, Promega; enzyme-to-substrate ratio 1:50) at 37°C overnight. After centrifugation, the supernatants were freeze dried, and the peptides were resolubilized in dissolving solution (0.1% formic acid, 2% acetonitrile). The peptides were separated on a Dionex UltiMate 3000 RSLCnano liquid chromatograph (Thermo Fisher Scientific) and identified on a Q Exactive mass spectrometer (Thermo Fisher Scientific). A 65-min liquid chromatography gradient (A = 0.1% formic acid, B = 0.1% formic acid, 80% acetonitrile) was used to separate the peptides at a flow rate of 300 nL/min. The peptides were identified from tandem MS spectra using ProteinPilot software 4.5 (v.1656) by searching against the rice database downloaded from RAP-DB. The proteins identified in *OsUBR7*^{OE}#9 seedlings were subtracted from the proteins identified in WT seedlings, and the results after filtering are detailed in Supplemental Data 1.

Expression and purification of recombinant proteins

Full-length coding sequences of target genes were cloned into corresponding vectors. Constructs of H2B point mutations (H2B_K136R, H2B_K144R, and H2B_K148R) were generated using a QuikChange site-directed mutagenesis kit (Stratagene, Santa Clara, CA, USA) according to the manufacturer's instructions.

The constructs were transferred into chemically-competent Rosetta (DE3) *E. coli* cells (TransGen Biotech, Beijing, China) for expression of recombinant proteins. The *E. coli* transformants were incubated in 100 mL Luria-Bertani liquid medium containing corresponding antibiotic at 37°C until they reached an optical density at 600 nm of 0.5. Then, 0.5 mM isopropyl-β-D-thiogalactoside was added and incubated at induction temperature for another 8 h to induce the production of recombinant protein. After harvesting by centrifugation, the pellet was resuspended in lysis buffer and lysed mildly for 10 min (4 s sonication/8 s rest) by ultrasonication, followed by binding to corresponding beads and washing with wash buffer. The recombinant proteins were eluted and analyzed by western blotting.

Western blotting

Protein extracts were separated by 12% SDS–polyacrylamide gel electrophoresis (PAGE) and transferred to nitrocellulose membranes (PALL) by semi-dry blotting in 15 mM Tris–HCl, 120 mM glycine, and 20% methanol. The membrane was blocked with non-fat dry milk in Tris-buffered saline (0.1% Tween-20). Blots were probed with specific primary antibodies and horseradish-peroxidase-conjugated secondary antibodies against mouse immunoglobulin G (TransGen Biotech HS201-01, 1:5000 dilution) and rabbit immunoglobulin G (TransGen Biotech HS101-01, 1:5000 dilution). Chemiluminescence detection was performed with an ECL kit (Amersham, Piscataway, NJ, USA) following the manufacturer's instructions.

GST pull-down assay

GST and GST-tagged proteins were incubated with MBP, MBP-tagged proteins, and His-tagged proteins in a lysis buffer at 4°C overnight. The complex was pulled down with glutathione Sepharose beads (Thermo Fisher Scientific), washed with lysis buffer, and analyzed using western blotting with specific antibodies against MBP (mouse, TransGen Biotech HT701-01, 1:5000 dilution), GST (mouse, TransGen Biotech HT601-01, 1:5000 dilution), and His (mouse, TransGen Biotech HT501-01, 1:5000 dilution). Ten percent of protein was used as input.

In vitro ubiquitination assay

The E2 Ub conjugation assay was adapted from a previous study (Zhao et al., 2013). In brief, the reaction was carried out in a total volume of 30 μL ubiquitinylation buffer at a final concentration of 50 mM Tris–HCl (pH 7.4), 10 mM $MgCl_2$, and 10 mM ATP. Purified 6×His-tagged Ub (His-AtUBQ14; 5 μg) was incubated with crude extract containing recombinant Arabidopsis E1 (His-AtUBA2) and 500 ng purified E2 (His-OsUBC18) at 30°C for 1 h.

For the various E2/E3 ubiquitination assays, reactions were performed following the manufacturer's protocol (Cat#: BML-UW9920, Enzo Life Sciences, Lausen, Switzerland) with a slight modification. The reaction was carried out in a total volume of 50 μL ubiquitinylation buffer at a final concentration of 50 mM Tris–HCl (pH 7.4), 1 U inorganic pyrophosphatase, 1 mM dithiothreitol (DTT), 10 mM $MgCl_2$, and 10 mM ATP. Purified 6×His-tagged Ub (5 μg) was incubated with crude extract containing recombinant Arabidopsis E1 (AtUBA2), 100 ng purified human E2s (for OsUBR7, OsUBC18 acts as the E2), and 1 μg purified 6×His-tagged E3 (OsUBR7), along with 1 μg purified MBP-tagged substrate (H2A, H2B, or point mutations of H2B) at 37°C for 1 to 3 h. The reactions were terminated by adding SDS sample buffer with DTT. The reaction products were separated by SDS–PAGE, blotted, and analyzed via western blotting with antibodies against Ub (mouse, Abcam ab7254, 1:2000 dilution), MBP, H2Aub1 (rabbit, Cell Signaling Technology 8240T, 1:1000 dilution), and H2Bub1 (rabbit, Cell Signaling Technology 5546T, 1:2000 dilution).

Histone extraction and detection of global H2Bub1 level

The procedure was adapted from a previous study (Charron et al., 2009) with a slight modification. Ten grams of seedlings ground in liquid nitrogen were homogenized in 20 mL histone extraction buffer (10 mM Tris–HCl [pH 7.5], 2 mM EDTA, 0.25 M HCl, 5 mM DTT, and protease inhibitor), filtered through a 500-mesh filter, and centrifuged for 20 min at 12 000 × *g* at 4°C. The supernatant was precipitated with 25% trichloroacetic acid, and the pellets were collected by centrifugation at 17 000 × *g* at 4°C for 30 min. The pellet was washed twice with ice-cold acetone, resuspended in Laemmli buffer, and dissolved overnight at room temperature.

The obtained histone extracts were separated by SDS–PAGE, blotted, and analyzed via western blotting. Global H2Bub1 levels were detected with anti-H2Bub1 antibody. Anti-H3 (rabbit, Cell Signaling Technology 4499T, 1:2000 dilution) immunoblotting was performed as a loading control. Relative band intensities of the immunoblots were calculated using ImageJ software.

ChIP-seq and data analysis

ChIP assays were performed as described previously by Wuhan Igenebook Biotechnology (http://www.igenebook.com). In brief, seedling samples (3 g each, two biological repeats) of WT Nipponbare and *osubr7* (in the Nipponbare background) were cross-linked in 1% formaldehyde under vacuum, and chromatin was extracted and fragmented by sonication. Next, anti-H2Bub1 antibody (rabbit, Cell Signaling Technology 5546S) and Dynabeads protein G (Cat#: 10004D, Invitrogen) were added to the

fragmented chromatin, followed by incubation overnight. Immunoprecipitated DNA was used to construct sequencing libraries following the protocol provided by the I NEXTFLEX ChIP-Seq Library Prep Kit for Illumina Sequencing (Bioo Scientific, Austin, TX, USA, NOVA-5143-02) and sequenced on the Illumina NovaSeq 6000 platform with the PE 150 method. Trimmomatic (v.0.38) was used to filter out low-quality reads. Clean reads were then mapped to the rice genome (IRGSP-1.0, https://rapdb.dna.affrc.go.jp/) with BWA (v.0.7.15). Samtools (v.1.3.1) was used to remove potential PCR duplicates. MACS2 (v.2.1.1.20160309) was used to call peaks with default parameters. If the summit of a peak was located closest to the transcription site of a gene, the peak was assigned to that gene. HOMER (v.3) was used with default settings to predict motif occurrence within peaks with a maximum motif length of 12 base pairs. GO enrichment analysis was performed using the EasyGO GO enrichment analysis tool (http://bioinformatics.cau.edu.cn/easygo/). GO-term enrichment was calculated using the hypergeometric distribution with a p value cutoff of 0.01. The p values obtained by Fisher's exact test were adjusted with a false discovery rate for multiple comparisons to detect overrepresented GO terms. Differential enrichment of peaks was identified using the R package DiffBind (v.2.16.0) with $p < 0.05$. H2Bub1-downregulated genes in *osubr7* compared with WT are detailed in Supplemental Data 2.

ChIP–qPCR analysis

ChIP–qPCR signals of the immunoprecipitated DNA and negative controls (no antibody) were normalized respectively by input DNA. Immunoprecipitation efficiency was defined as the resultant value of immunoprecipitated DNA minus the background value of the negative control. According to the results of ChIP-seq, the *OsNRAMP2* gene without a change in H2Bub1 level was used as an internal chromatic gene control. The amounts of immunoprecipitated DNA were assayed by qPCR using the same conditions as qRT–PCR.

Transcriptome analysis

Transcriptome sequencing was carried out using 21-day-old seedlings of WT Nipponbare and *osubr7* (in the Nipponbare background). The Trizol method was used to isolate total RNA from the seedlings. Transcriptome sequencing was carried out by Genedenove Corporation (Guangzhou, China). Genes whose expression was downregulated in *osubr7* relative to the WT were identified using a threshold of $\geq$2-fold change in expression with $p \leq 0.05$, and the results are detailed in Supplemental Data 3.

Analyses of haplotype, H_p, and fixation index

Haplotypes of the *OsUBR7* promoter and CDS regions were analyzed using 1491 *japonica* and 3019 *indica* accessions from the RiceVarMap v.2.0 database (http://ricevarmap.ncpgr.cn/hap_net/) (Zhao et al., 2021) and 98 wild rice accessions from the OryzaGenome2.1 database (http://viewer.shigen.info/oryzagenome21detail/index.xhtml) (Kajiya-Kanegae et al., 2021). The analysis results are detailed in Supplemental Data 5.

F_{ST} between these *japonica* and *indica* accessions on a chromosomal sweep (10-kb scanning window with a 5-kb step) and individual SNPs was calculated using VCFtools (Danecek et al., 2011). The H_p of individual SNPs at *OsUBR7* in these accessions was analyzed as described previously (Wang et al., 2021).

For association analysis, the plant height data of 527 rice accessions were downloaded from the RiceVarMap2 database. After filtering haplotypes that occurred in less than 2.5% of all accessions, 503 accessions for CDS haplotype analysis and 455 accessions for promoter haplotype analysis remained. These accessions were divided into five dominant CDS haplotypes (cH1–cH5) and five dominant promoter haplotypes (pH1–pH5).

Nuclei isolation and flow cytometry

Basal 3-mm segments of 7-day-old seedlings were finely chopped into pieces with sharp blades and incubated in 0.3 mL nuclei extraction buffer (Ref#: 05-5002-P02, Sysmex Partec, Görlitz, Sachsen, Germany) for 1 min. The homogenate was then filtered through a 400-mesh filter, and 1.2 mL staining buffer (Ref#: 05-5002-P01, Sysmex Partec) was added and incubated for 1 min. The nuclei suspension was loaded into a CyFlow Space flow cytometer (Sysmex Partec), and the ploidy of approximately 50 000 nuclei was recorded for each test. The numbers of diploid and tetraploid nuclei were recorded, and the relative proportions of G1-, S-, and G2/M-phase cells were calculated using ModFit LT software (v.4.1.7).

Statistical analysis

For observations of agronomic traits, measurement of cell length, cell-cycle-related measurements, and gene expression analyses (qRT–PCR), statistical analyses were conducted in Excel as detailed in the figure legends (Supplemental Data 7).

ACCESSION NUMBERS

Sequence data from this article can be found at RAP-DB (https://rapdb.dna.affrc.go.jp), TAIR (https://www.arabidopsis.org), or HGNC (https://www.genenames.org) under the following accession numbers: *OsUBR7* (*Os06g0529800*), *OsUBC18* (*Os09g0293400*), *OsH2A* (*Os07g0545300*), *OsH3* (*Os03g0390600*), *OsH4* (*Os10g0539500*), *OsH2B.1* (*Os03g0279000*), *OsH2B.2* (*Os08g0490900*), *OsH2B.3* (*Os01g0149400*), *OsH2B.4* (*Os01g0149600*), *OsH2B.5* (*Os01g0153300*), *OsH2B.6* (*Os01g0153100*), *OsH2B.7* (*Os01g0152900*), *OsH2B.9* (*Os05g0574300*), *OsH2B.10* (*Os01g0152300*), *OsH2B.11* (*Os01g0839500*), *AtUBA2* (*At5g06460*), *AtUBQ14* (*At4g02890*), *UBR7* (*HGNC:20344*), *UbcH5b* (*HGNC:12475*), and *H2B.1* (*HGNC:4751*).

SUPPLEMENTAL INFORMATION

Supplemental information is available at *Plant Communications Online*.

FUNDING

This work was supported by the Major Program of Guangdong Basic and Applied Basic Research (2019B030302006), the National Natural Science Foundation of China (31921004, 31871533, and 31760300), the Laboratory of Lingnan Modern Agriculture Project (NT2021002), and the Guangdong Basic and Applied Basic Research Foundation (2019A1515010230).

AUTHOR CONTRIBUTIONS

Y.-G.L. and Y.Z. designed the research; Y.Z., Y.L., and S.Z. performed the experiments; Y.Z. analyzed the data; Y.-G.L., Y.Z., and Z.C. wrote the manuscript.

ACKNOWLEDGMENTS

We are grateful to Professor Qi Xie for providing the vectors for the *in vitro* ubiquitination assay. No conflict of interest is declared.

Received: April 20, 2022
Revised: June 20, 2022
Accepted: July 8, 2022
Published: July 14, 2022

REFERENCES

Adhikary, S., Chakravarti, D., Terranova, C., Sengupta, I., Maitituoheti, M., Dasgupta, A., Srivastava, D.K., Ma, J., Raman, A.T., Tarco, E., et al. (2019). Atypical plant homeodomain of UBR7 functions as an H2BK120Ub ligase and breast tumor suppressor. Nat. Commun. **10**:1398.

Ahmad, A., Zhang, Y., and Cao, X.F. (2010). Decoding the epigenetic language of plant development. Mol. Plant **3**:719–728.

Bae, H., and Kim, W.T. (2014). Classification and interaction modes of 40 rice E2 ubiquitin-conjugating enzymes with 17 rice ARM-U-box E3 ubiquitin ligases. Biochem. Biophys. Res. Commun. **444**:575–580.

Braun, S., and Madhani, H.D. (2012). Shaping the landscape: mechanistic consequences of ubiquitin modification of chromatin. EMBO Rep. **13**:619–630.

Briggs, S.D., Xiao, T., Sun, Z.W., Caldwell, J.A., Shabanowitz, J., Hunt, D.F., Allis, C.D., and Strahl, B.D. (2002). Gene silencing: trans-histone regulatory pathway in chromatin. Nature **418**:498.

Cai, H., Xiao, J., Zhang, Q., and Lian, X. (2010). Co-suppressed glutamine synthetase2 gene modifies nitrogen metabolism and plant growth in rice. Chin. Sci. Bull. **55**:823–833.

Caplan, J., Padmanabhan, M., and Dinesh-Kumar, S.P. (2008). Plant NB-LRR immune receptors: from recognition to transcriptional reprogramming. Cell Host Microbe **3**:126–135.

Cesari, S., Bernoux, M., Moncuquet, P., Kroj, T., and Dodds, P.N. (2014). A novel conserved mechanism for plant NLR protein pairs: the "integrated decoy" hypothesis. Front. Plant Sci. **5**:606.

Charron, J.B.F., He, H., Elling, A.A., and Deng, X.W. (2009). Dynamic landscapes of four histone modifications during deetiolation in *Arabidopsis*. Plant Cell **21**:3732–3748.

Chen, C., Chen, H., Zhang, Y., Thomas, H.R., Frank, M.H., He, Y., and Xia, R. (2020). TBtools: an integrative toolkit developed for interactive analyses of big biological data. Mol. Plant **13**:1194–1202.

Chen, L., Shiotani, K., Togashi, T., Miki, D., Aoyama, M., Wong, H.L., Kawasaki, T., and Shimamoto, K. (2010). Analysis of the Rac/Rop small GTPase family in rice: expression, subcellular localization and role in disease resistance. Plant Cell Physiol. **51**:585–595.

Chen, S., Tao, L., Zeng, L., Vega-Sanchez, M.E., Umemura, K., and Wang, G.L. (2006). A highly efficient transient protoplast system for analyzing defence gene expression and protein-protein interactions in rice. Mol. Plant Pathol. **7**:417–427.

Chi, Y.H., Moon, J.C., Park, J.H., Kim, H.S., Zulfugarov, I.S., Fanata, W.I., Jang, H.H., Lee, J.R., Lee, Y.M., Kim, S.T., et al. (2008). Abnormal chloroplast development and growth inhibition in rice thioredoxin m knock-down plants. Plant Physiol. **148**:808–817.

Christensen, D.E., Brzovic, P.S., and Klevit, R.E. (2007). E2-BRCA1 RING interactions dictate synthesis of mono- or specific polyubiquitin chain linkages. Nat. Struct. Mol. Biol. **14**:941–948.

Cui, H., Tsuda, K., and Parker, J.E. (2015). Effector-triggered immunity: from pathogen perception to robust defense. Annu. Rev. Plant Biol. **66**:487–511.

Danecek, P., Auton, A., Abecasis, G., Albers, C.A., Banks, E., DePristo, M.A., Handsaker, R.E., Lunter, G., Marth, G.T., Sherry, S.T., et al. (2011). The variant call format and VCFtools. Bioinformatics **27**:2156–2158.

Zhiguo, E., Zhang, Y., Li, T., Wang, L., and Zhao, H. (2015). Characterization of the ubiquitin-conjugating enzyme gene family in rice and evaluation of expression profiles under abiotic stresses and hormone treatments. PLoS One **10**:e0122621.

Ferrero-Serrano, Á., Cantos, C., and Assmann, S.M. (2019). The role of dwarfing traits in historical and modern agriculture with a focus on rice. Cold Spring Harb. Perspect. Biol. **11**:a034645.

Frankham, R., Briscoe, D.A., and Ballou, J.D. (2002). Introduction to Conservation Genetics (Cambridge University Press).

Fuchs, G., Shema, E., Vesterman, R., Kotler, E., Wolchinsky, Z., Wilder, S., Golomb, L., Pribluda, A., Zhang, F., Haj-Yahya, M., et al. (2012). RNF20 and USP44 regulate stem cell differentiation by modulating H2B monoubiquitylation. Mol. Cell **46**:662–673.

Gaur, V.S., Channappa, G., Chakraborti, M., Sharma, T.R., and Mondal, T.K. (2020). 'Green revolution' dwarf gene *sd1* of rice has gigantic impact. Brief. Funct. Genomics **19**:390–409.

Gibson, D.G. (2011). Enzymatic assembly of overlapping DNA fragments. Methods Enzymol. **498**:349–361.

Han, J., Ma, K., Li, H., Su, J., Zhou, L., Tang, J., Zhang, S., Hou, Y., Chen, L., Liu, Y.G., et al. (2022). All-in-one: a robust fluorescent fusion protein vector toolbox for protein localization and BiFC analyses in plants. Plant Biotechnol. J. **20**:1098–1109. https://doi.org/10.1111/pbi.13790.

He, G., Elling, A.A., and Deng, X.W. (2011). The epigenome and plant development. Annu. Rev. Plant Biol. **62**:411–435.

Hedden, P. (2003). The genes of the green revolution. Trends Genet. **19**:5–9.

Joo, H.Y., Zhai, L., Yang, C., Nie, S., Erdjument-Bromage, H., Tempst, P., Chang, C., and Wang, H. (2007). Regulation of cell cycle progression and gene expression by H2A deubiquitination. Nature **449**:1068–1072.

Kajiya-Kanegae, H., Ohyanagi, H., Ebata, T., Tanizawa, Y., Onogi, A., Sawada, Y., Hirai, M.Y., Wang, Z.X., Han, B., Toyoda, A., et al. (2021). OryzaGenome2.1: database of diverse genotypes in wild *Oryza* species. Rice **14**:24.

Kleiner, R.E., Hang, L.E., Molloy, K.R., Chait, B.T., and Kapoor, T.M. (2018). A chemical proteomics approach to reveal direct protein-protein interactions in living cells. Cell Chem. Biol. **25**:110–120.e3.

Komatsu, K., Maekawa, M., Ujiie, S., Satake, Y., Furutani, I., Okamoto, H., Shimamoto, K., and Kyozuka, J. (2003). LAX and SPA: major regulators of shoot branching in rice. Proc. Natl. Acad. Sci. USA **100**:11765–11770.

Kouzarides, T. (2007). Chromatin modifications and their function. Cell **128**:693–705.

Hu, Y., and Lai, Y. (2015). Identification and expression analysis of rice histone genes. Plant Physiol. Biochem. **86**:55–65.

Liu, C., Zheng, S., Gui, J., Fu, C., Yu, H., Song, D., Shen, J., Qin, P., Liu, X., Han, B., et al. (2018). Shortened basal internodes encodes a gibberellin 2-Oxidase and contributes to lodging resistance in rice. Mol. Plant **11**:288–299.

Liu, L., Michowski, W., Kolodziejczyk, A., and Sicinski, P. (2019). The cell cycle in stem cell proliferation, pluripotency and differentiation. Nat. Cell Biol. **21**:1060–1067.

Liu, W., Xie, X., Ma, X., Li, J., Chen, J., and Liu, Y.G. (2015). DSDecode: a web-based tool for decoding of sequencing chromatograms for genotyping of targeted mutations. Mol. Plant **8**:1431–1433.

Longbotham, J.E., Chio, C.M., Dharmarajan, V., Trnka, M.J., Torres, I.O., Goswami, D., Ruiz, K., Burlingame, A.L., Griffin, P.R., and Fujimori, D.G. (2019). Histone H3 binding to the PHD1 domain of histone demethylase KDM5A enables active site remodeling. Nat. Commun. **10**:94.

Ma, X., Zhang, Q., Zhu, Q., Liu, W., Chen, Y., Qiu, R., Wang, B., Yang, Z., Li, H., Lin, Y., et al. (2015). A robust CRISPR/Cas9 system for convenient, high-efficiency multiplex genome editing in monocot and dicot plants. Mol. Plant **8**:1274–1284.

Monna, L., Kitazawa, N., Yoshino, R., Suzuki, J., Masuda, H., Maehara, Y., Tanji, M., Sato, M., Nasu, S., and Minobe, Y. (2002). Positional cloning of rice semidwarfing gene, sd-1: rice "green revolution gene" encodes a mutant enzyme involved in gibberellin synthesis. DNA Res. **9**:11–17.

Niu, M., Wang, Y., Wang, C., Lyu, J., Wang, Y., Dong, H., Long, W., Wang, D., Kong, W., Wang, L., et al. (2017). ALR encoding dCMP deaminase is critical for DNA damage repair, cell cycle progression and plant development in rice. J. Exp. Bot. **68**:5773–5786.

Polge, C., Cabantous, S., Deval, C., Claustre, A., Hauvette, A., Bouchenot, C., Aniort, J., Béchet, D., Combaret, L., Attaix, D., et al. (2018). A muscle-specific MuRF1-E2 network requires stabilization of MuRF1-E2 complexes by telethonin, a newly identified substrate. J. Cachexia Sarcopenia Muscle **9**:129–145.

Ramanathan, H.N., and Ye, Y. (2012). Cellular strategies for making monoubiquitin signals. Crit. Rev. Biochem. Mol. Biol. **47**:17–28.

Richly, H., Rocha-Viegas, L., Ribeiro, J.D., Demajo, S., Gundem, G., Lopez-Bigas, N., Nakagawa, T., Rospert, S., Ito, T., and Di Croce, L. (2010). Transcriptional activation of polycomb-repressed genes by ZRF1. Nature **468**:1124–1128.

Robinson, P.A., and Ardley, H.C. (2004). Ubiquitin-protein ligases. J. Cell Sci. **117**:5191–5194.

Sasaki, A., Ashikari, M., Ueguchi-Tanaka, M., Itoh, H., Nishimura, A., Swapan, D., Ishiyama, K., Saito, T., Kobayashi, M., Khush, G.S., et al. (2002). Green revolution: a mutant gibberellin-synthesis gene in rice. Nature **416**:701–702.

She, K.C., Kusano, H., Koizumi, K., Yamakawa, H., Hakata, M., Imamura, T., Fukuda, M., Naito, N., Tsurumaki, Y., Yaeshima, M., et al. (2010). A novel factor FLOURY ENDOSPERM2 is involved in regulation of rice grain size and starch quality. Plant Cell **22**:3280–3294.

Siqueira, J.A., Hardoim, P., Ferreira, P.C.G., Nunes-Nesi, A., and Hemerly, A.S. (2018). Unraveling interfaces between energy metabolism and cell cycle in plants. Trends Plant Sci. **23**:731–747.

Spielmeyer, W., Ellis, M.H., and Chandler, P.M. (2002). Semidwarf (sd-1), "green revolution" rice, contains a defective gibberellin 20-oxidase gene. Proc. Natl. Acad. Sci. USA **99**:9043–9048.

Springer, N.M., and Schmitz, R.J. (2017). Exploiting induced and natural epigenetic variation for crop improvement. Nat. Rev. Genet. **18**:563–575.

Sriram, S.M., Kim, B.Y., and Kwon, Y.T. (2011). The N-end rule pathway: emerging functions and molecular principles of substrate recognition. Nat. Rev. Mol. Cell Biol. **12**:735–747.

Tasaki, T., and Kwon, Y.T. (2007). The mammalian N-end rule pathway: new insights into its components and physiological roles. Trends Biochem. Sci. **32**:520–528.

Tasaki, T., Mulder, L.C.F., Iwamatsu, A., Lee, M.J., Davydov, I.V., Varshavsky, A., Muesing, M., and Kwon, Y.T. (2005). A family of mammalian E3 ubiquitin ligases that contain the UBR box motif and recognize N-degrons. Mol. Cell Biol. **25**:7120–7136.

Tasaki, T., Sriram, S.M., Park, K.S., and Kwon, Y.T. (2012). The N-end rule pathway. Annu. Rev. Biochem. **81**:261–289.

van Wijk, S.J.L., de Vries, S.J., Kemmeren, P., Huang, A., Boelens, R., Bonvin, A.M.J.J., and Timmers, H.T.M. (2009). A comprehensive framework of E2-RING E3 interactions of the human ubiquitin-proteasome system. Mol. Syst. Biol. **5**:295.

Ve, T., Williams, S.J., and Kobe, B. (2015). Structure and function of Toll/interleukin-1 receptor/resistance protein (TIR) domains. Apoptosis **20**:250–261.

Wang, M., Chen, J.H., Zhou, F., Yuan, J.M., Chen, L.B., Wu, R.L., Liu, Y.G., and Zhang, Q.Y. (2021). The Ties of Brotherhood between *Japonica* and *Indica* Rice for Regional Adaptation (Science China-Life Sciences).

Wang, Y., and Li, J. (2008). Molecular basis of plant architecture. Annu. Rev. Plant Biol. **59**:253–279.

Wang, Z., Liang, Y., Li, C., Xu, Y., Lan, L., Zhao, D., Chen, C., Xu, Z., Xue, Y., and Chong, K. (2005). Microarray analysis of gene expression involved in anther development in rice (Oryza sativa L.). Plant Mol. Biol. **58**:721–737.

Weake, V.M., and Workman, J.L. (2008). Histone ubiquitination: triggering gene activity. Mol. Cell **29**:653–663.

Wojcik, F., Dann, G.P., Beh, L.Y., Debelouchina, G.T., Hofmann, R., and Muir, T.W. (2018). Functional crosstalk between histone H2B ubiquitylation and H2A modifications and variants. Nat. Commun. **9**:1394.

Worden, E.J., Hoffmann, N.A., Hicks, C.W., and Wolberger, C. (2019). Mechanism of cross-talk between H2B ubiquitination and H3 methylation by Dot1L. Cell **176**:1490–1501.e12.

Xie, X., Ma, X., Zhu, Q., Zeng, D., Li, G., and Liu, Y.G. (2017). CRISPR-GE: a convenient software toolkit for CRISPR-based genome editing. Mol. Plant **10**:1246–1249.

Xu, C., and He, C. (2007). The rice *OsLOL2* gene encodes a zinc finger protein involved in rice growth and disease resistance. Mol. Genet. Genomics. **278**:85–94.

Yaish, M.W., El-Kereamy, A., Zhu, T., Beatty, P.H., Good, A.G., Bi, Y.M., and Rothstein, S.J. (2010). The APETALA-2-like transcription factor OsAP2-39 controls key interactions between abscisic acid and gibberellin in rice. PLoS Genet. **6**:e1001098.

Yamamuro, C., Ihara, Y., Wu, X., Noguchi, T., Fujioka, S., Takatsuto, S., Ashikari, M., Kitano, H., and Matsuoka, M. (2000). Loss of function of a rice brassinosteroid insensitive1 homolog prevents internode elongation and bending of the lamina joint. Plant Cell **12**:1591–1606.

Yuan, Z., Luo, D., Li, G., Yao, X., Wang, H., Zeng, M., Huang, H., and Cui, X. (2010). Characterization of the *AE7* gene in *Arabidopsis* suggests that normal cell proliferation is essential for leaf polarity establishment. Plant J. **64**:331–342.

Zhang, Y., Li, D., Zhang, H., Hong, Y., Huang, L., Liu, S., Li, X., Ouyang, Z., and Song, F. (2015). Tomato histone H2B monoubiquitination enzymes SlHUB1 and SlHUB2 contribute to disease resistance against Botrytis cinerea through modulating the balance between SA- and JA/ET-mediated signaling pathways. BMC Plant Biol. **15**:252.

Zhang, Y., Song, G., Lal, N.K., Nagalakshmi, U., Li, Y., Zheng, W., Huang, P.-j., Branon, T.C., Ting, A.Y., Walley, J.W., et al. (2019). TurboID-based proximity labeling reveals that UBR7 is a regulator of N NLR immune receptor-mediated immunity. Nat. Commun. **10**:3252.

Zhao, H., Li, J., Yang, L., Qin, G., Xia, C., Xu, X., Su, Y., Liu, Y., Ming, L., Chen, L.L., et al. (2021). An inferred functional impact map of genetic variants in rice. Mol. Plant **14**:1584–1599.

Zhao, Q., Tian, M., Li, Q., Cui, F., Liu, L., Yin, B., and Xie, Q. (2013). A plant-specific in vitro ubiquitination analysis system. Plant J. **74**:524–533.

Zhao, W., Neyt, P., Van Lijsebettens, M., Shen, W.H., and Berr, A. (2019). Interactive and noninteractive roles of histone H2B monoubiquitination and H3K36 methylation in the regulation of active gene transcription and control of plant growth and development. New Phytol. **221**:1101–1116.

Zhao, Z., Zhang, Z., Ding, Z., Meng, H., Shen, R., Tang, H., Liu, Y.G., and Chen, L. (2020). Public-transcriptome-database-assisted selection and validation of reliable reference genes for qRT-PCR in rice. Sci. China Life Sci. **63**:92–101.